Artificial Recharge of Groundwater, Peters et al. (eds) © 1998 Balkema, Rotterdam, ISBN 90 5809 017 5

Quality changes upon injection into anoxic aquifers in the Netherlands: Evaluation of 11 experiments

Pieter J. Stuyfzand
Kiwa Research and Consultancy, Nieuwegein, Netherlands

ABSTRACT: Since 1973 11 deep well recharge experiments, each at a different site with intensive hydrochemical monitoring, were carried out in the Netherlands. At each test site the influent was oxic and the anoxic target aquifer contained pyrite. All experiments revealed a typical quality evolution in 7 phases due to sequential leaching of aquifer constituents. The main processes were, in mean order of increasing duration: mixing with native groundwater, cation exchange, SiO_2 desorption, PO_4 and F exchange, pyrite oxidation, acid-buffering by calcite dissolution or HCO_3^-, and oxidation of organic matter. Differences in quality changes between the experiments relate to variations in aquifer geochemistry and influent quality. Pyrite oxidation is kinetically hindered, it takes about 10-100 days to deplete O_2 and NO_3^- in the influent. Oxygen is reacting faster with pyrite than with labile organic matter, for nitrate the reverse holds. Pyrite oxidation leads to mobilization of As, Co, Ni and Zn, of which only As may reach the recovery well.

1 INTRODUCTION

In the past 25 years, 11 independent experiments with deep well recharge and intensive hydrochemical monitoring were carried out in the Netherlands (Fig.1). These experiments aimed at getting insight into (a) the feasibility of recharging confined aquifers with surface water through wells, for drinking water supply, and (b) the resulting water quality changes, because these have consequences for pre- and post-treatment and effects on clogging of the recharge and recovery wells. The general driving force was an increasing demand for drinking water, in areas where the government forced the water supply companies to restrict their groundwater pumping, in order to combat the drawdown of groundwater tables and to restore wetlands in selected areas. In most cases oxic water was prepared from surface water (by partial purification or by full treatment to drinking water standards; Table 1), and was subsequently injected into a deep anoxic, sandy aquifer and recovered by a pumping well at 75-200 m distance. In this contribution the hydrochemical results of the experiments are compared and integrated to provide general patterns in the quality evolution downgradient and with time.

2 SITES AND METHODS

The experiments were carried out in various environments (Fig.1): the coastal dunes (1-6), the Rhine fluvial plain (7-9) and Pleistocene uplands (10-11). Some details on the 11 experiments, of which number 6 (with 24 injection wells) is actually part of a current drinking water production system, are listed in Table 1.

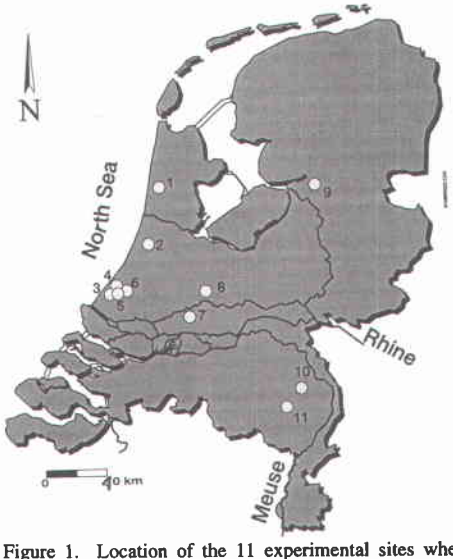

Figure 1. Location of the 11 experimental sites where oxic water was or still is injected into an anoxic aquifer, with intensive hydrochemical monitoring.

Table 1. Some details on the 11 experiments with deep well injection of oxic water into an anoxic aquifer. The locations are shown in Fig.1 (MSL = Mean Sea Level).

site no	site name	Water Supply Company	period of injection	source injection water @	injection depth m-MSL	injection rate m^3/h	target aquifer m-MSL	geologic formation**	number sampled wells	anal. program water#	further data in §
1	Castricum AIP	PWN	75-77	Y_p	81-90	10-30	41-102	En	2	MC	
2	Leiduin WIP	GW	76-77	$R_{d,p}$	22-36	30	14-74	E,D	9	MC	a
3	Scheveningen DIP	DZH	73-80	R_d,M_d	25-45	37-60	20-53	E,U/S	2	MC	b
4	Scheveningen CIP	DZH	74-77	R_p,M_p	23-42	36	11-47	E,U/S	3	MC	
5	Scheveningen F/F	DZH	84-88	M_p	29-42	15-20	27-44	E,U/S	4	All	i
6	Waalsdorp	DZH	90-date	M_p	25-63	20	23-67	E,U/S	3	All	
7	Langerak	WZHO	96-98	G_{d+t}	73-92	35	68-93	K,H	13	MC,TE	c,d,e,j
8	Nieuwegein	WZHO	96-98	R_p	104-132	40	90-136	K,H	10	MC,TE,P	c,j
9	St. Jansklooster	WMO	96-97	G_d	48-85	28-53	22-110	En,H	9	MC,TE,P	f
10	Breehei	WML	94-95	G_{d+t}	15-26	26	5-28	Ki	10	MC,TE	
11	Someren DIZON	WOB	96-98	Z_p	257-284	30	248-287	Ki	22	MC,TE	g,h

@: G = local groundwater; M = river Meuse water; R = river Rhine water; Y = lake IJsselmeer water; Z = canal water from Zuid-Willemsvaart; d = treated to drinking water; p = pretreated (half fabricate); t = NaCl and $NaNO_3$ added.
**: D = Drenthe Formation (glacial); E = Eemian Formation (marine); En = Enschede Formation (fluvial); H = Harderwijk Formation (fluvial); K = Kedichem Formation (fluvial); Ki = Kiezeloolite Formation (fluvial); U/S = Urk or Sterksel formation (fluvial).
#: All = MC + TE + organic micropollutants; MC = Main Constituents; P = Parallel column; TE = Trace Elements.
§: a = Appelo et al. 1979; b = Van Beek & Van Puffelen 1986; c = Timmer & Stuyfzand 1998; d = Saaltink et al. 1998; e = Brun et al. 1998; f = De Ruiter & Stuyfzand 1998; g = Straatman & Brekvoort 1998; h = Stuyfzand 1998; i = Rutte 1990; j = Stuyfzand & Timmer 1998.

Quality monitoring consisted of frequent analysis of: (a) the oxic influent, (b) groundwater from observation wells at various distances from the recharge well, and (c) the percolate of parallel columns filled with aquifer cores and flushed with injection water on site (only sites 8-9). Most monitoring wells were situated along the shortest flow paths between injection and recovery well. Groundwater samples were obtained by suction lift from PVC-piezometers (well screen 1-2 m long). The water content of riser plus well screen was purged 3 times prior to sampling. Temperature, EC, pH and O_2 were measured on site. Alkalinity, pH and EC were measured in the laboratory, on the day of sampling. The portion to be analyzed for most trace elements, Ca^{2+}, Mg^{2+}, Fe, Mn, SiO_2 and PO_4 (both ortho and total) was filtrated in situ over 0.45 µm, directly acidified to pH=1,5 using HNO_3-suprapure and was stored in the dark at 4 °C in polyethylene vessels rinsed out with HNO_3 and the water to be sampled. Main constituents were analysed with conventional, well-standardized analytical methods, most trace elements were analyzed using Atomic Absorption Spectrophotometry (AAS) with graphite furnace.

In 7 experiments sediment cores from the target aquifer were obtained using a core catcher during bailer drilling of the monitoring wells. The sediment cores including their pore water were immediately sealed on site using liquidized paraffin, and kept at 4°C in the dark till analysis. Samples were opened and pretreated in an anoxic glove-box since 1996. The samples were analysed for amongst others: total content of 27 elements by X-Ray Fluorescence, organic matter and calcium carbonate by thermogravimetry (resp. 550 and 1000°C), $CaCO_3$ by HCl-extraction of Ca^{2+} (correcting for exchangeable Ca; ppm level), organic carbon by pyrolysis, exchangeable cations using $SrCl_2$, sulphide species (especially pyrite) with a sequential extraction, non-Si-bound trace elements by aqua regia extraction and amorphous Al-, Fe- and Mn-(hydr)oxides by ammonium oxalate/oxalic acid.

3 THE ORIGINAL SITUATION

3.1 *Hydro(geo)logy*

The target aquifers are composed of Pleistocene sands (1-9) or Miocene sands (10-11), in most cases with a modal grain size of 300-500 µm and 0.5-2% <2 µm (clay fraction) and 0-3% >2 mm (gravel). The resulting permeability is in most cases 30-50 m/d, porosity varies from 29-35%. In all cases the recharged sediments exhibit, within the scale of about 100 m (horizontal) by 30 m (vertical), a significant heterogeneity especially in vertical direction. In all cases the target aquifer is (semi)confined.

3.2 *Hydrochemistry*

In most cases the native groundwater in the target aquifer was fresh (Cl^- 7-70 mg/l), calcite saturated (pH 6.6-7.6, Ca^{2+} 40-100 mg/l) and either anoxic (no oxygen, no nitrate, sulphate (meta)stable) or deep anoxic (no oxygen, no nitrate, no sulphate), with relatively high concentrations of Fe^{2+} (1-10 mg/l), Mn^{2+} (0.1-0.6 mg/l), NH_4^+ (0.3-5 mg/l), SiO_2 (18-40 mg/l) and, exclusively in deep anoxic water (sites 1, 2, 7-10), methane (2-32 mg/l).

Table 2. Survey of mean geochemistry of the various geological formations which were flushed by oxic water during deep well recharge. The experimental site numbers correspond with those in Table 1 and Fig.1.

Geol. code	Formation name§	exper. site no.	fraction <2 µm %	mean grain size µm	CEC meq/kg	$CaCO_3$ mg/kg	organic carbon % d.w.	FeS_2 as S mg/kg	Fe_{EXCH} (calc) meq/kg	$NH_{4\text{-}EXCH}$ (calc) meq/kg	$Fe(OH)_3$ as Fe mg/kg
Pleistocene Formations											
E	Eemian^{Ma}	2-6	0.9	350	9.0	45,000	0.11	220	0.55	0.05	-
D	Drenthe^{G}	2	-	325	-	≤10,000	≤0.1	-	-	-	-
U/S	Urk^{R}/Sterksel^{RMe}	3-6	0.8	340	8.0	17,500	0.09	230	0.10	0.10	-
En	Enschede^{E}	9	0.5	450	4.5	<50	0.05	440	0.14	0.45	30
K/H	Kedichem/H^{ER}:U	7,8	3.9	240	24.0	18,160	0.14	225	0.34	0.20	1,085
H/K	Harderwijk/K^{E}:M+L	7	1.4	360	9.5	5,600	0.12	160	0.19	0.07	1,020
H/K	Harderwijk/K^{E}:M+L	8	0.6	390	6.7	1,360	0.08	65	0.04	0.03	570
Miocene formations											
Ki	Kieseloölite^{R}:U	10-11	1.7	330	68	≤200	0.8	4,520	1.07	0.05	525
	Kieseloölite^{R}:M+L	10-11	0.8	350	10	<200	0.4	700	0.30	0.03	≤9

§: L = Lower part; M = Middle part; U = Upper part; $_{E}$ = fluvial, origin in NE-Germany; $_{G}$ = glacial; $_{Ma}$ = marine; $_{Me}$ = fluvial, river Meuse; $_{R}$ = fluvial, river Rhine;

Within each target aquifer some vertical hydrochemical stratification was noticed, often connected to the vertical sedimentary stratification.

3.3 *Geochemistry*

The chemical composition of the 11 target aquifers varied especially in connection with the geological formation (Table 1) and within each formation in connection with the clay fraction (<2 µm) or mean grain size. The mean characteristics of the discerned formations are listed in Table 2.

Most formations contain (very) low amounts of very reactive pyrite. Calcium carbonate is typically present in marine deposits and Pleistocene sediments deposited by the river Rhine, and practically absent in deposits from ancient rivers with an eastern provenance and in Rhine deposits of Miocene age. Calcium was in all cases the dominant exchangeable cation (58-82% of CEC; 37% on site 1), followed by resp. Mg^{2+} (6-26%; 33% on site 1), Na^{+} (1-8%; 22% on site 1), K^{+} (1-6%; 8% on site 1), Fe^{2+} (1-6%), NH_4^{+} (0.2-2%; 11% on site 9) and Mn^{2+} (0.1-0.4%). The content of exchangeable Fe^{2+}, Mn^{2+} and NH_4^{+} was calculated (as measurements were always biased by oxygenation) according to a procedure described by Stuyfzand & Timmer 1998.

The maximum trace element content of pyrite was estimated by linear regression of As, Co, Ni and Zn (as extracted with aqua regia) with pyrite. On site 7 and 8 the following stoichiometry was thus deduced for these fluvial sediments:

$Fe_{0.98}Co_{0.0037}Ni_{0.01}Zn_{0.01}S_2As_{0.0053}$.

Several aquifers are suspected to contain manganous siderites ($Fe_{1-x}Mn_xCO_3$) in small amounts. Their quantification and reactivity are matter for future research.

4 QUALITY AND TRACING OF INFLUENT

4.1 Quality

The mean quality of the water injected, is shown in Table 3. On sites 2, 3, 4, 7 and 10 there were important changes during the experiment, due to either taking another water source (2, 3, 4, 10) or stopping the addition of NaCl and $NaNO_3$ (7,10). Where drinking water was used (2, 3, 7, 9, 10) only minor quality and temperature fluctuations occurred, contrary to the sites receiving pretreated surface water.

Iron, Mn, PO_4 and CH_4 (not shown in Table 3), were in general <0.05 mg/L. High SiO_2 concentrations (19-21 mg/L) are connected with groundwater, moderate levels with drinking water prepared from surface water by basin recharge and recovery (10-13 mg/L) and low contents with pretreated surface water (2-5 mg/L). The extremely low DOC levels on sites 8 (1.3 mg/L) and 11 (0.8 mg/L) are caused by filtration over activated granular carbon as part of the pretreatment.

Important parameters for behaviour during aquifer passage, are the calcite saturation index (SI_c = log $[Ca^{2+}][CO_3^{2-}]/K_{CaCO3}$) and the Modified Oxidation Capacity (MOC), a modification of the 'oxidation capacity of water' as introduced by Broers et al. 1991. MOC is explained in footnote '§' of Table 3; the modifications include the assumption of stable behaviour of sulphate (without oxidation capacity), and a correction for oxidizable compounds in the influent itself (100% nitrification of ammonium and, based on numerous observations, 20% oxidation of DOC). It should be noted that MOC is in milli-electrons/L, and that the oxidation of 1 mmol of pyrite and organic matter lower MOC by resp. 15 and 4 me/L.

Table 3. Mean quality of the water injected.

site no	name	type @	EC µS/cm	temp °C	pH -	O_2 mg/L	Cl mg/L	SO_4^{2-} mg/L	HCO_3^- mg/L	NO_3^- mg/L	Ca^{2+} mg/L	NH_4^+ mg/L	DOC mg/L	SiO_2 mg/L	MOC me/L	SI_c -
1	Castricum	Y_p	1100	9.5	7.95	11	220	135	130	7	96	0.03	5.7	2	1.55	0.26
2	Leiduin	R_d	966	9.5	8.0	7.1	180	75	213	6	92	0.05	2.3	12.9	1.21	0.53
		R_p	840	13	7.6	4.2	150	73	160	22	81	0.06	3.0	5	2.09	0.03
3	Schev. DIP	R_d	910	12.4	7.61	8.1	169	83	191	8.5	96	0.03	2.8	10	1.51	0.16
		M_d	630	11.5	7.76	9.4	89	69	198	7.3	80	0.04	3.6	10	1.52	0.25
4	Schev. CIP	R_p	950	12.0	7.40	8.0	180	80	140	14	80	0.10	3.5	4	1.88	-0.26
		M_p	660	12.0	7.40	9.0	85	95	160	15	80	0.17	4.0	4	2.04	-0.20
5	Schev. F/F	M_p	580	12.3	7.08	9.5	81	75	144	15.0	76	0.03	2.8	3.7	2.21	-0.56
6	Waalsdorp	M_p	586	13.0	7.32	10.0	73	78	146	15.1	72	<0.03	2.3	3.5	2.31	-0.33
7	Langerak	G_{d+t}	700	13.5	7.7	9.5	92	8	298	14.9	60.2	0.02	3.0	20	2.19	0.34
		G_d	470	11.0	7.6	9.5	11	8	298	14.9	60.2	0.02	3.0	20	2.19	0.34
8	Nieuwegein	R_p	746	13.7	7.57	5.7	126	63	158	14.9	74.5	0.03	1.3	4	1.82	-0.02
9	St. Janskl.	G_d	499	11.9	7.51	9.9	38	11	265	9.2	85.2	0.06	7.2	19.1	1.49	0.17
10	Breehei	G_{d+t}	425	11.5	7.65	10.5	51	10	185	11	52	<0.05	4.2	20	1.92	-0.02
		G_d	290	11.5	7.45	8.9	13	6	176	1	54	<0.05	4.2	19	0.91	-0.22
11	Someren	Z_p	557	12.0	7.12	9.9	82	62	117	19.2	68.4	0.07	0.8	3.4	2.72	-0.60

@: G = local groundwater; M = river Meuse water; R = river Rhine water; Y = lake IJsselmeer water; Z = canal water from Zuid-Willemsvaart; d = treated to drinking water; p = pretreated (half fabricate); t = NaCl and $NaNO_3$ added.
§: MOC = $4(O_2 - 2\,NH_4^+) + 5(NO_3^- + NH_4^+) - 0.8$ DOC, with concentrations in mmol/L, MOC in me/L.

The range in SI_c is from -0.60 (calcite agressive; site 11) to +0.53 (calcite supersaturated; site 2 first period). The range in MOC is from 0.9 (site 10 second period) to 2.7 me/L (site 11).

4.2 Tracing

Chloride, electrical conductivity, temperature, sulphate, methane and hydrogencarbonate proved to be very useful tracers of the injection water. Although only chloride behaves as a perfectly conservative tracer, the others were conservative enough for use (see methane in Fig.2).
With temperature a retardation factor of 2.0 ± 0.1 should be taken into account due to heat exchange with the aquifer matrix (Olsthoorn 1981; Stuyfzand 1997). At the Langerak site where sodium chloride was added for a short time (30 days), sulphate (high in influent) and methane (low in influent) were especially useful for the recovery well where dispersion of the tracer added and mixing with native groundwater faded away the initial chloride contrast (Stuyfzand & Timmer 1998).
The break-through at levels in between observation screens was established using (a) 0.01 °C accurate temperature sounding in the deepest piezometer prior to any pumping for sampling, and (b) resistivity measurements (of formation plus groundwater; latter variable) with fixed electrodes, both on a frequent basis.
The mean travel time (t_{50}) is defined as 50% break-through, and is used to calculate for each observation the amount of pore flushes (PFs) with the injection water during the injection period (Δt_{inj}): $PF = \Delta t_{inj}/t_{50}$.

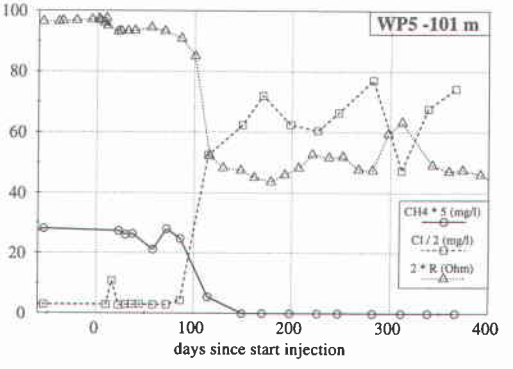

Figure 2. The break-through curves of chloride and methane (in groundwater sampled with a 1 meter long well screen) and of the electrical resistivity (measured with a fixed electrode couple in gravel pack of well) yield about the same mean travel time for observation well WP5-101 (site 8) and longitudinal dispersivity: resp. 105 days and 0.3 m.

5 GENERALIZED QUALITY CHANGES

The water quality changes of oxic water upon anoxic aquifer passage generally evolve in a specific way with time, due to sequential leaching of reactive components of the aquifer matrix. The quality evolution of the main constituents is shown for a calcareous aquifer in Fig.3. The patterns shown are based on numerous observations at test sites 1-8, with emphasis on sites 5-6. The evolution reveals 7 phases, which are discussed below in

order of increasing number of pore flushes (PFs). The number of PFs for phases 3-6 is only approximative and holds for water with a travel time of 3-10 days (most data). The first break-through of nitrate and sulphate, initiating resp. phases 3 and 4, requires less PFs for water with a shorter travel time due to the relatively slow kinetics of redox reactions. As the available data contain time series up to 400 PFs, the further evolution is based on calculations using the transport code EASY-LEACHER (Stuyfzand 1998). Of course, the evolution depicted is only valid for a more or less continuous injection without clogging or with an easily curable clogging.

Phase 1: displacement (0.5-1.5 PFs)

During this initial phase the native groundwater is displaced by the water injected. Both fluids mix due to dispersion by both the porous medium and the sampling with 1-2 m long well screens. The longitudinal dispersivity, as derived from break-through curves, in fact combines both mixing mechanisms and is about 0.5-1 m for most sands. Close to the injection well this mixing will result in typical reactions like the precipitation of ferrihydroxides and manganous oxides, as well as nitrification. These precipitation reactions do not pose clogging problems because (a) clogging was never observed in the beginning of injection and (b) the reactants oxygen and nitrate in the injection water are soon used up by redox reactions making the front of injection water totally anoxic.

Phase 2: cation exchange and sorption (1.5-7 PFs)

Exchange and sorption reactions between influent and aquifer matrix dominate during the second phase. In most cases Na^+ and especially Ca^{2+} expel part of the adsorbed K^+, Mg^{2+}, NH_4^+, Fe^{2+} and Mn^{2+} from the exchangers (reaction 13 in Table 4), while SiO_2 and PO_4^{3-} desorb (reactions 14-15 in Table 4), and F^- adsorbs (reaction 16 in Table 4).
A general order of increasing duration of the exchange or sorption can be given for several constituents, with the PFs within brackets (see also Table 6): Na^+ (1.5-2) < Mg^{2+} (6) < NH_4^+ (7) < SiO_2 (7-8) < K^+ (8) < PO_4^{3-} (14).
Sodium, K^+ and Mg^{2+} do not have other sources and sinks; the abundant silicate minerals are practically inert due to approximate saturation of the influent and the relatively short travel times (maximum 100-500 days). Desorption is the main source of NH_4^+ and PO_4^{3-}. The oxidation of solid phase Natural Organic Matter (NOM) constitutes in some cases a minor source of both, whereas calcite and calciumphosphates may form an additional phosphate source in some cases. Desorbing NH_4^+ can be nitrified by oxygen, and phosphate may sorb to neoformed ironhydroxides.

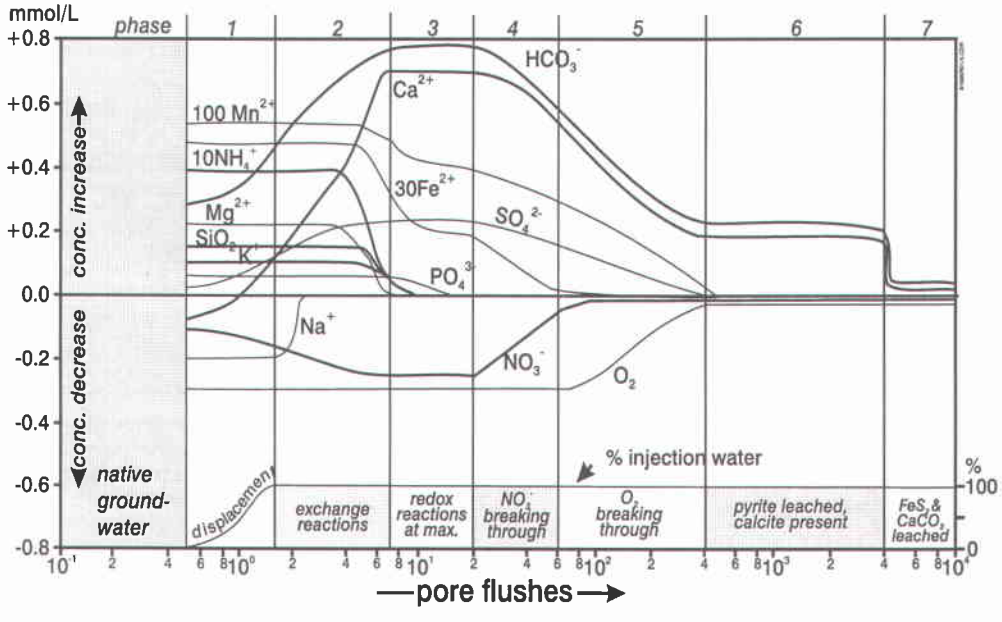

Figure 3. Generalized evolution of the quality changes of oxic injection water in an anoxic, calcareous aquifer, as a function of the number of pore flushes of the soil in between injection and observation well (modified after Stuyfzand 1989). The X-axis also gives the retardation factor for species with a negative change, and the leach factor for species with a positive change.

This apparently speeds up the leaching process. Silica mainly derives from adsorbed SiO_2 (Bassett, in Wood & Signor 1975), but also amorphous SiO_2 (like diatom skeletons) may dissolve especially in marine formations. The behaviour of Fe^{2+} and Mn^{2+} is not dictated by desorption alone but also by redox reactions and possibly the dissolution of a manganous siderite. During phase 2, redox reactions (discussed below) and calcite dissolution rapidly grow to full size. However, in various cases some lag develops probably due to adaptation of the microbiological population, which is needed to catalyze oxidation processes.

Phase 3: redox reactions at maximum (7-20 PFs)

Redox reactions are quantitatively the most important reactions, which also trigger acid buffering reactions like the dissolution of calcite. The maximum size of redox reactions is reached when O_2 and NO_3^- are completely consumed, and when SO_4^{2-}, TIC (= Total Inorganic Carbon = CO_2 + HCO_3^-) and Ca^{2+} (in case $CaCO_3$ is buffering the acid produced) reach their maximum concentration. This moment is in general already reached after 1.5-7 PFs, so that phase 3 may overlap phase 2. The size of both the redox reactions and calcite dissolution declines when nitrate is breaking through in phase 4. Using the mass balance approach the water-aquifer interactions could be simulated very satisfactorily with O_2 mainly reacting with pyrite (mainly reaction 5a, also reaction 5b), and NO_3^- mainly with NOM (largely reaction 8a, reaction 8b in traces). The best lead in quantifying pyrite oxidation is sulphate, which is produced and does not have other sources and sinks. Some nitrate or, only in specific layers low in NOM and high in pyrites, all nitrate is used for pyrite oxidation as well. The main reaction product of NOM-oxidation is HCO_3^-, which is obscured, however, by a much larger HCO_3^- source in case of calcite dissolution (reaction 17 in Table 4), and by a HCO_3^- sink (reaction 21 in Table 4) in case $CaCO_3$ is lacking.

Phase 4: nitrate breaking through (20-60 PFs)

The first break-through of nitrate initiates phase 4, which is characterized by a slowly increasing redox potential in consequence of a steady NO_3^- increase. This is probably connected with the depletion of: (a) the most labile fractions of NOM and, to a smaller degree, pyrite; and (b) mobilized Fe^{2+} (from desorption and pyrite oxidation). As a matter of fact the increasing NO_3^- levels are mirrored by decreasing Fe^{2+} concentrations. This may be partly connected with mixing reaction 4a in Table 4. Also Ca^{2+}, HCO_3^- and Mn^{2+} are declining but less dramatically than Fe^{2+}.

Phase 5: oxygen breaking through (60-400 PFs)

When the front of pyrite leaching is approaching, oxygen will break through which heralds phase 5. The oxygen concentrations do either rise slowly (Fig.3) or more abruptly, probably depending on the width of the pyrite leaching zone. The behaviour of oxygen is typically followed by decreasing SO_4^{2-}, Ca^{2+} and HCO_3^- concentrations. Nitrate removal and iron mobilization may approach zero after about 80 PFs.

Phase 6: pyrite consumed (400-4,000 PFs)

When sulphate stops to increase, pyrite is completely consumed or at least the reactive pyrite particles. This is the start of phase 6. It is calculated for sites 1-8 and also demonstrated by observations, that calcite is still present at this stage. Now the main reactions in the aquifer are dominated by the oxidation of NH_4^+ and DOC in the influent, and by the calcite saturation index of the influent. The latter is assumed in this generalization to be negative, implying a calcite agressive influent. In most cases there still is a less reactive NOM fraction which consumes oxygen or nitrate at a very slow rate.

Phase 7: pyrite/calcite consumed (>4,000 PFs)

At this stage the CO_2 produced by oxidation reactions (NH_4^+ and DOC in the influent and NOM in aquifer matrix) and the negative calcite saturation index of the influent, are not buffered any more by calcite dissolution. This results in minor quality changes during aquifer passage, with a small pH decrease and small increase in TIC.

6 COMPARING SITES 1-11

The water quality changes and evolution patterns at the 11 sites are compared in Table 5. Most conspicuous are the differences in the parameter $\Delta C/\Delta S$, which is the ratio of the mean molar change in HCO_3^- and SO_4^{2-} as observed during phase 3 of aquifer passage. As ΔSO_4 is positive on each site, a positive value indicates HCO_3^- production and a negative value HCO_3^- consumption. Pyrite oxidation by O_2 according to reaction 5a (Table 4) yields in combination with calcite dissolution $\Delta C/\Delta S = +2$. And pyrite oxidation by NO_3^- according to reaction 6b (Table 4) yields in combination with calcite dissolution $\Delta C/\Delta S = +0.5$.
Values >+2.5 therefore point at a significant HCO_3^- production by calcite dissolution in connection with a negative calcite saturation index (SI_c) of the influent or denitrification by NOM.

Table 4. Listing of important reactions between on the one hand the injected water and native groundwater (upon mixing), and on the other hand injected water and solid constituents of the target aquifer.

Reactions upon mixing

$O_2 + 4\ Fe^{2+} + 8\ HCO_3^- + 2\ H_2O \rightarrow 4\ Fe(OH)_3 + 8\ CO_2$ (1)

$2\ O_2 + NH_4^+ + 2\ HCO_3^- \rightarrow NO_3^- + 2\ CO_2 + 3\ H_2O$ (2)

$0.5\ O_2 + Mn^{2+} + 2\ HCO_3^- \rightarrow MnO_2 + 2\ CO_2$ (3)

$0{,}2\ NO_3^- + Fe^{2+} + 1{,}8\ HCO_3^- + 0{,}6\ H_2O \rightarrow Fe(OH)_3 + 0{,}1\ N_2 + 1{,}8\ CO_2$ (4a)

$NO_2^- + 3\ Fe^{2+} + 5\ HCO_3^- + 2\ H_2O \rightarrow 0{,}5\ N_2 + 3\ Fe(OH)_3 + 5\ CO_2$ (4b)

Reactions with pyrite and NOM

$3{,}75\ O_2 + FeS_2 + 4\ HCO_3^- \rightarrow Fe(OH)_3 + 2\ SO_4^{2-} + 4\ CO_2 + 0{,}5\ H_2O$ (5a)

$3{,}5\ O_2 + FeS_2 + 2\ HCO_3^- \rightarrow Fe^{2+} + 2\ SO_4^{2-} + 2\ CO_2 + H_2O$ (5b)

$2{,}8\ NO_3^- + FeS_2 + 0{,}8\ H^+ \rightarrow Fe^{2+} + 2\ SO_4^{2-} + 1{,}4\ N_2 + 0{,}4\ H_2O$ (6a)

$3\ NO_3^- + FeS_2 + HCO_3^- + H_2O \rightarrow Fe(OH)_3 + 2\ SO_4^{2-} + 1{,}5\ N_2 + CO_2$ (6b)

$O_2 + CH_2O \rightarrow CO_2 + H_2O$ (7)

$NO_3^- + 1{,}25\ CH_2O \rightarrow 0{,}5\ N_2 + 0{,}25\ CO_2 + HCO_3^- + 0{,}75\ H_2O$ (8a)

$NO_3^- + 0{,}5\ CH_2O \rightarrow NO_2^- + 0{,}5\ CO_2 + 0{,}5\ H_2O$ (8b)

Other redox reactions

$MnO_2 + 0{,}5\ CH_2O + 1{,}5\ CO_2 + 0{,}5\ H_2O \rightarrow Mn^{2+} + 2\ HCO_3^-$ (9)

$Fe(OH)_3 + 0{,}25\ CH_2O + 1{,}75\ CO_2 \rightarrow Fe^{2+} + 2\ HCO_3^- + 0{,}75\ H_2O$ (10)

$O_2 + 4\ FeCO_3 + 6\ H_2O \rightarrow 4\ Fe(OH)_3 + 4\ CO_2$ (11)

$NO_3^- + 5\ FeCO_3 + 8\ H_2O \rightarrow 5\ Fe(OH)_3 + \frac{1}{2}N_2 + HCO_3^- + 4\ CO_2$ (12)

Exchange reactions

$[Fe,NH_4,Mn,K,Mg]\text{-EXCH} + Ca^{2+} + Na^+ \leftrightarrow [Ca,Na]\text{-EXCH} + Fe^{2+} + NH_4^+ + Mn^{2+} + K^+ + Mg^{2+}$ (13)

$[H_4SiO_4]\text{-EXCH} + X \leftrightarrow [X]\text{-EXCH} + H_4SiO_4$ (14)

$[H_2PO_4]\text{-EXCH} + HCO_3^- \leftrightarrow [HCO_3]\text{-EXCH} + H_2PO_4^-$ (15)

$[OH]\text{-EXCH} + F^- + CO_2 \leftrightarrow [F]\text{-EXCH} + HCO_3^-$ (16)

Dissolution/precipitation and pH-buffering

$CaCO_3 + H_2CO_3 \leftrightarrow Ca^{2+} + 2\ HCO_3^-$ (17)

$Fe_{1-x}Mn_xCO_3 + H_2CO_3 \leftrightarrow 1\text{-}x\ Fe^{2+} + x\ Mn^{2+} + 2\ HCO_3^-$ (18)

$SiO_2 + 2H_2O \rightarrow H_4SiO_4$ (19)

$Fe(OH)_3 + x\ H_4SiO_4 + H_2O \leftrightarrow Si_xFe(OH)_{3+4x} \cdot H_2O$ (20)

$H^+ + HCO_3^- \leftrightarrow H_2CO_3 \leftrightarrow CO_2 + H_2O$ (21)

$CaCO_3$ = calcite; CH_2O = organic matter; EXCH = exchanger; $Fe(OH)_3$ = ironhydroxide; $FeCO_3$ = siderite; FeS_2 = pyrite; H_4SiO_4 = dominant silicon species dissolved in water.

Finally, negative $\Delta C/\Delta S$ values indicate internal acid buffering by HCO_3^- which then converts to CO_2 (reaction 21 in Table 4). Now the $\Delta C/\Delta S$ values in combination with the SI_c values and calcite content of the aquifer (Table 5) reveal 3 groups:

(a) sites 1-6 and 8 (site 2 with $SI_c = 0.03$) where calcite dissolved in significant amounts;

(b) sites 2 (with $SI_c = 0.53$) and 7 (with $SI_c = 0.34$) where calcite is present but not dissolving due to supersaturation and where $\Delta C/\Delta S$ is negative; and

(c) sites 9-11 where calcite is lacking and the negative $\Delta C/\Delta S$ indicates acid buffering by HCO_3^-.

As expected, group a also shows high leach factors (up to >400) for both Ca^{2+} and HCO_3^-, whereas groups b and c display low values (1.5-16).

The parameter $f\Delta SO_4$ is defined as the ratio of the observed change in SO_4^{2-} during phase 3 of aquifer passage and the calculated, potential maximum change of SO_4 (being in mmoles: 2*MOC/15). It is deduced from Table 5 that site 2 has an exceptionally low value (0.1), and that sites 5, 7 (only lower part of aquifer), 9 and 11 (only lower part of aquifer) display a relatively high value (≥0.65), pointing at resp. a low and high capture efficiency of oxidants by pyrite. This is probably connected with differences in the amount and reactivity of labile NOM and labile pyrite. A small size of pyrite crystals and the absence of coatings (especially by NOM) raise $f\Delta SO_4$.

There is an exceptionally fast, low-level breakthrough for nitrate only at sites 2, 10 and 11 ($R_{10\%}$ <2), whereas oxygen is showing there a normal retarded, low-level break-through ($R_{10\%}$ >33 up to >146). This indicates a very low reactivity of the NOM, which in case of sites 10-11 can be attributed to the relatively high age of the Miocene sands as compared to the Pleistocene aquifers on the other sites. The fast nitrate break-through combines with a relatively low leach factor for Fe^{2+} (4-7 compared with 14-≥73).

Sites 2, 9, 10 and probably 7 (not measured) are unique regarding the behaviour of SiO_2: its concentration drops below the relatively high influent level (which is only little lower than in the native groundwater). This excludes the normal sorptive behaviour which is observed elsewhere. It is assumed that SiO_2 coprecipitates with neoformed $Fe(OH)_3$ according to reaction 20 (Table 4). Only at site 2 this SiO_2 removal was overshadowed for a short period by a strong desorption. The sites in the coastal dunes (1-6) display a relatively high leach factor for K^+ (8-27 versus 5-7). This is probably connected with previous salt water flushing of these coastal aquifers, which is also manifested by raised K^+ concentrations in the fresh dune water today.

Table 5. Comparison of the water quality changes c.q. leaching and retardation factors upon injection of oxic water into an anoxic aquifer at 11 sites, for observation points with a travel time of 3-10 days. R_X = retardation factor for X = t_X/t_{50}; L_X = leach factor for X = t_X/t_{50}, with t_{50} = 50% breakthrough of conservative tracer like Cl^-; t_X = time for 10 or 90% breakthrough of solute X (if influent higher than native groundwater then retardation, otherwise leaching).

site no	name	SI_c @	$CaCO_3$† %	$\Delta C/\Delta S$ #	$f\Delta SO_4$ ##	R_{O2} 10-90%§	R_{NO3} 10-90%§	L_K 90%	L_{Mg} 90%	L_{NH4} 90%	L_{Fe} 90%	L_{Mn} 90%	L_{SiO2} 90%	L_{PO4} 90%	L_{Ca} 90%	L_{HCO3} 90%
1	Castricum	+0.26	>1	+2.6	0.5	27->102	18-102	14	11	11	32	80	11	15	>140	>140
2	Leiduin	+0.53	5	-3.2	0.1	>14	1->14	>14	9	9	2-13	>14	6	13	5^R	1.5
		+0.03	5	+5.0	0.1	>69	1-69	27	-	-	-	>69	-	-	>69	>69
3	Schev. DIP	+0.20	2.5	+3.1	0.6	140->244	<22-109	-	-	-	38	94	-	-	>244	>244
4	Schev. CIP	-0.23	2.5	+6.3	0.4	<240->400	<40-100	-	-	-	>40	>40	-	-	>400	>400
5	Schev. F/F	-0.56	2.5	+5.7	0.7	49-95	14-83	12	7	5	≥73	≥95	10	24	>95	>95
6	Waalsdorp	-0.33	2.5	+5.0	0.6	>49	>49	8	6	8.5	>49	>49	7	-	>49	>49
7	Langerak	+0.34	0.65	-0.3	0.4/0.9[a]	>61	24->61	$6^{R/L}$	$4^{R/L}$	14	14->57	31->57	-	-	$\leq 3^R$	1.5
8	Nieuwegein	-0.02	0.8	+3.8	0.35	24->114	1->114	5	5	7	14	>114	-	-	>114	>114
9	St. Janskl.	+0.17	≤0.002	-1.1	0.7	>95	>26	6^R	5.5^R	5	21	>26	$>26^R$	14	1.5	1.5
10	Breehei	-0.12	≤0.013	-1.2	0.4	>33	2->15	$7^{R/L}$	$10^{R?L}$	11	4	26	$>10^R$	-	4^R	1-16
11	Someren	-0.60	<0.02	-1.4	0.4/0.7[a]	>146	1-43	-	≤2	6	7	17	4	-	-	-

@ = calcite saturation index of influent; † = mean calcite content of target aquifer; § = if one value, then for both 10 and 90%.
R = retardation; R/L = retardation and leaching on different levels in aquifer; a: X/Y = (upper + middle)/(lower part of aquifer);
#: $\Delta C/\Delta S$ = ratio of mean molar change in HCO_3^- and SO_4^{2-} as observed during aquifer passage (ΔSO_4 always positive);
##: $f\Delta SO_4$ = ratio of observed SO_4^{2-} change during aquifer passage and the calculated potential maximum SO_4 change (being in mmoles: 2*MOC/15).

7 SOME DETAILS ON PYRITE OXIDATION

Pyrite oxidation which was observed on all test sites, can be considered as the most important water-sediment reaction. This reaction proved to be kinetically hindered on all sites (Fig.4), which corresponds with Nicholson et al. (1988, 1990). It is concluded from Fig.4 that it takes about 10-100 days to use up the O_2 and NO_3^- in the influent for pyrite oxidation, and that 40-100% of the oxidants is actually consumed exclusively by pyrite oxidation. Saaltink et al. (1998) modelled pyrite oxidation for site 7, including reaction kinetics.

Where denitrification by NOM is important, an inverse behaviour of O_2 and ΔSO_4, and of NO_3^- and HCO_3^- was observed.

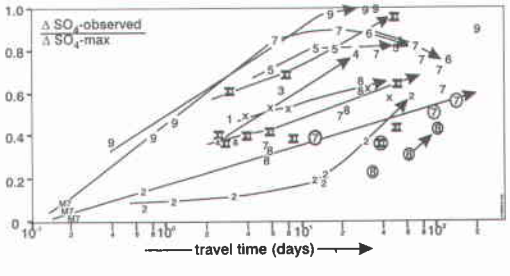

Figure 4. The oxidation of pyrite is a relatively slow process taking about 10-100 days to deplete O_2 and NO_3^- in the influent. The reaction progress variable is the observed sulphate increase (ΔSO_4), which is plotted here for phase 3 (redox reactions at maximum) as the ratio to the maximum potential sulphate increase (ΔSO_4-max = 2*MOC/15). This ratio is denominated $f\Delta SO_4$ in Table 5. The numbers indicate the test site, interconnected numbers are situated along a flow path, and encircled numbers are those with an anomalously high denitrification by natural organic matter.

This indicates that oxygen is reacting faster with pyrite than with labile NOM, and that the reverse holds for nitrate. The rate of pyrite oxidation further depends on temperature as demonstrated in Fig.5. When temperature drops below ca. 10°C the reaction slows down considerably.

The oxidation of pyrite leads to some mobilization of As, Co and Ni, as shown in Fig.6. This is consistent with the geochemical composition of pyrite (section 3). Zinc did not mobilize, however, possi-

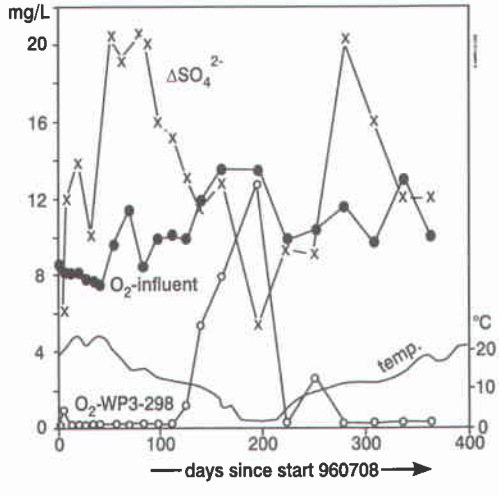

Figure 5. The temperature dependency of pyrite oxidation in observation well WP3-298 at test site 11 (distance to injection well 8 m, travel time 3 days), is manisfested by oxygen and the sulphate increase ($\Delta SO_4 = (SO_4^{2-})_{WP3\text{-}298} - (SO_4^{2-})_{influent}$).

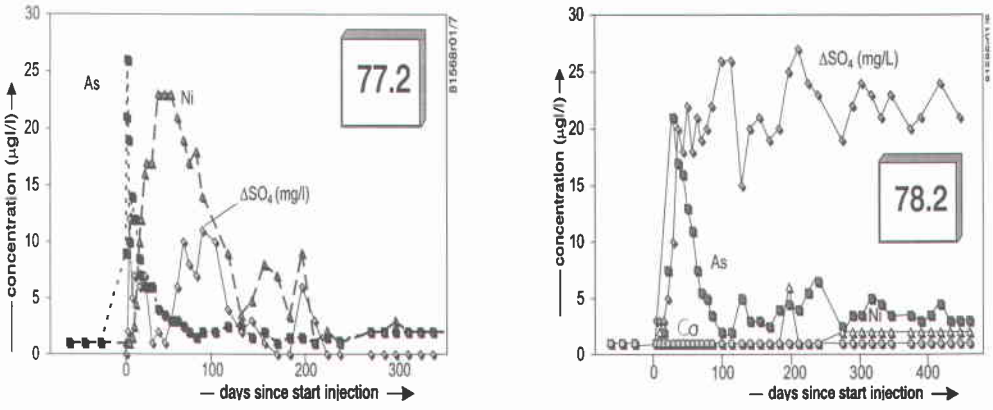

Figure 6. Relation between the observed sulphate increase (ΔSO_4) and the concentrations of As, Co and Ni in observation wells WP.77-60 and WP.78-60 at test site 9 (distance to injection well resp. 3 and 33 m, travel time resp. 0.5 and 21 days).

bly due to a more effective scavenging by neoformed $Fe(OH)_3$. Cobalt and Ni are clearly much less mobile than As which is noticed further away from the injection well. These metals probably coprecipitate with or strongly adsorb to the neoformed $Fe(OH)_3$. Arsenic is initially more mobile due to its reduced state (occurring in water as H_3AsO_3) which prevents it to sorb to $Fe(OH)_3$. After some time the advancing oxygen and nitrate fronts converse the dissolving arsenic into the oxidized state (AsO_4^{3-}) which is much less mobile due to preferential sorption to neoformed $Fe(OH)_3$.

REFERENCES

Appelo, C.A.J., P.J. Stuyfzand & G.B. Engelen 1979. Reactions of Rhine water in the Veluwe and dunes: an experimental study and an injection test. *H_20* 12 (in dutch), 328-332.

Broers, H.P., J. Griffioen & E.A. Buijs 1994. Rela tions between groundwater and sediment composition for 5 well sites in N. Brabant. TNO-report OS.94-38-A, 90p.

Brun, A., F.D. Christensen, J.S. Christiansen, P.J. Stuyfzand & H. Timmer 1998. Water quality modelling at the Langerak deep-well recharge site. This volume.

De Ruiter, H. & P.J. Stuyfzand 1998. An experiment on deep well recharge of oxic water into an anoxic aquifer near St. Jansklooster. This volume.

Nicholson, R.V., R.W. Gillham & E.J. Reardon 1988. Pyrite oxidation in carbonate-buffered solution: 1. Experimental kinetics. *Geochim. Cosmochim. Acta* 52, 1077-1085.

Nicholson, R.V., R.W. Gillham & E.J. Reardon 1990. Pyrite oxidation in carbonate-buffered solution: 2. Rate control by oxide-coatings. *Geochim. Cosmochim. Acta* 54, 395-402.

Olsthoorn, T.N. 1982. Clogging of recharge wells. Kiwa-Meded. 71 (in dutch).

Postma, D., C. Boesen, H. Kristiansen & F. Larsen 1991. Nitrate reduction in an unconfined sandy aquifer: water chemistry, reduction processes and geochemical modeling. *Water Resources Research* 27, 2027-2045.

Saaltink, M.W., C. Ayora, P.J. Stuyfzand & H. Timmer 1998. Modelling the effects of deep artificial recharge on groundwater quality. This volume.

Straatman, R. & Y. Brekvoort 1998. Well recharge pilot South-East Netherlands, this volume.

Stuyfzand, P.J. 1989. Comparing artificial recharge using basins and wells on a geohydrochemical basis. *H_2O* 22, 721-728.

Stuyfzand, P.J. 1998. Simple models for reactive transport of pollutants and main constituents during artificial recharge and bank filtration. This volume.

Stuyfzand, P.J. & H. Timmer 1998. Injecting oxic surface water into an anoxic aquifer along the river Rhine; water-rock interactions including redox dynamics. Kiwa-report EU-contract ENV4-CT95-0071, in prep.

Timmer, H. & P.J. Stuyfzand 1998. Deep well re charge in a polder near the Rhine. This volume.

Van Beek, C.G.E.M. & J. Van Puffelen 1987. Changes in the chemical composition of drinking water after well infiltration in an unconsolidated sandy aquifer. *Water Resources Research* 23, 69-76.

Wood, W.W. & D.C. Signor 1975. Geochemical factors affecting artificial groundwater recharge in the unsaturated zone. *Transactions ASAE* 18, 677-683.